

# Deposition of organic-based superhydrophobic films for anti-adhesion and self-cleaning applications

On-Uma Nimitrakoolchai, Sitthisuntorn Supothina\*

National Metal and Materials Technology Center, 114 Thailand Science Park, Paholyothin Road, Klong Luang, Pathumthani 12120, Thailand

Available online 24 October 2007

## Abstract

Surface having superhydrophobic and self-cleaning property is generally found in nature such as lotus leaf and butterfly's wing. Such surfaces consist of protrusions in micrometer scale covered with waxy nanoparticles, giving the surface self-cleaning property as water droplets roll off the rough surface and pick up dirt and fine debris with them. Synthetic superhydrophobic films having similar feature have been fabricated for specific functions as water-repellence, self-cleaning and anti-fouling. This present work attempts to mimic such natural surface feature by controlling surface roughness of the underlying organic layer simply by chemical etching, followed by deposition of oxide nanoparticles and finally thin layer of organic molecules to further lower surface energy. The fabricated films on glass substrate exhibited water contact angle higher than 150°. Results of surface analysis by using an atomic force microscopy as well as results of self-cleaning and anti-adhesion are presented.

© 2007 Elsevier Ltd. All rights reserved.

**Keywords:** Superhydrophobic; Self-cleaning; Anti-adhesion; Lotus effect; Atomic force microscopy

## 1. Introduction

Surfaces having high hydrophobic and exhibiting water repellent properties are generally found in nature such as plant leaves and butterfly's wing. According to the study of Neinhuis and Barthlott,<sup>1</sup> there are more than 200 plant species of which the surfaces exhibited water repellent property. The water repellency is based on surface roughness caused by different microstructures, together with the hydrophobic property of wax crystals. The best-known example of a superhydrophobic self-cleaning surface is the lotus (*Nelumbo nucifera*) leaves. It consists of double-scaled roughness; about 10- $\mu\text{m}$  protruding nubs which are about 10–30  $\mu\text{m}$  apart covered with tiny wax crystal of about 0.2–2  $\mu\text{m}$ .<sup>1</sup> Such feature makes the surface superhydrophobic. When water drops roll off the leaf surfaces, they carry off dirt, leaving the surface perfectly clean.

Synthetic superhydrophobic self-cleaning surface was fabricated by mimicking the surface features found in nature to utilize its specific functions such as water repellency,<sup>2,3</sup> anti-adhesion<sup>4</sup> and anti-fouling.<sup>5</sup> Techniques used for preparation of superhydrophobic surface can be simply classified into two categories.<sup>6</sup> One is making a rough surface from a low surface

energy material.<sup>7–10</sup> The materials having low surface energy used to make superhydrophobic surface are fluorocarbons, silicones and organic materials (polyethylene, polystyrene, etc.) and inorganic materials (ZnO and TiO<sub>2</sub>). The other is modifying a rough surface with a material of low surface energy. There are many ways to make rough surfaces such as mechanical stretching, laser/plasma/chemical etching,<sup>5,11</sup> lithography,<sup>12</sup> sol-gel processing and self-assembly,<sup>13</sup> layer-by-layer and colloidal assembly.<sup>14</sup>

This present work attempts to mimic such natural surface feature by enhancing surface roughness of the underlying organic film simply by chemical etching, followed by deposition of silicon oxide (SiO<sub>2</sub>) nanoparticles and finally a thin film of organic molecules to create finer-scaled roughness and to lower surface energy, respectively.

## 2. Experimental procedure

### 2.1. Preparation of superhydrophobic film

Preparation of the superhydrophobic film on glass substrate consisted of two successive steps: deposition of an underlying polyelectrolyte film on the glass substrate followed by deposition of SiO<sub>2</sub> nanoparticles and silane molecules. Before deposition, the glass substrate was ultrasonically cleaned with

\* Corresponding author. Tel.: +66 2 5646447; fax: +66 2 5646447.  
E-mail address: [sitthis@mttc.or.th](mailto:sitthis@mttc.or.th) (S. Supothina).

ethanol, acetone and de-ionized water, respectively, and then dried at 60 °C in the oven. The polyelectrolyte film was deposited on the substrate by modifying the procedure of Zhai et al.<sup>14</sup> The cleaned substrate was coated with aqueous solutions of 0.02 M poly(allylamine hydrochloride) (PAH; molecular weight of 70,000; Aldrich) and 0.02 M poly(acrylic acid) (PAA; 35 wt% in H<sub>2</sub>O; molecular weight of 100,000; Aldrich) by a layer-by-layer deposition using a dip coater. The PAH layer was deposited by dipping the substrate in PAH solution (adjusted to pH of 8.7 using 1 M NaOH) for 15 min and then rinsing twice with de-ionized water. Then, the PAA layer was deposited by dipping the PAH-coated substrate in PAA solution (pH 3.3) for 15 min followed by rinsing with de-ionized water. This dipping cycle was repeated twice to obtain three PAH/PAA layers or three bilayers. The total of three bilayers was selected as it gave sufficient thickness for acid etching to create open porosity or roughness on the surface.

Desired surface roughness was obtained by etching the three bilayers polyelectrolyte film in HCl solutions having pH of 2.3 and 1.1, respectively so as to create the pore with diameters at micrometer scale at the surface of the polyelectrolyte film. Etching was performed for various immersion times (15, 60, 180 and 420 min) to alter surface roughness of the underlying polyelectrolyte film. The etched film was heated at 180 °C for 2 h. Then, SiO<sub>2</sub> nanoparticles having particle size of 40–45 nm were deposited onto the etched multilayer film by dipping it into a suspension of fumed SiO<sub>2</sub> (Aerosil 200,

JJ degussa). The SiO<sub>2</sub> suspension was prepared by ultrasonically mixing 0.06 g of fumed SiO<sub>2</sub> in 100 mL of de-ionized water. Finally, the sample was dipped in a solution of 0.4 vol% in 1-propanol of trichloro(1*H*,1*H*,2*H*,2*H*-perfluorooctyl) silane (CF<sub>3</sub>(CF<sub>2</sub>)<sub>5</sub>CH<sub>2</sub>CH<sub>2</sub>SiCl<sub>3</sub>, 97%; Aldrich) followed by cross-linking at 180 °C for 2 h.

## 2.2. Characterization

Surface topography was imaged by using an SPA 400 atomic force microscopy (AFM) performed in a non-contact mode. A root mean square (RMS) roughness was obtained from AFM image analysis. The RMS roughness was calculated according to the following equation:

$$\text{RMS} = \sqrt{\frac{\sum_{i=1}^N (Z_i - Z_{\text{av}})^2}{N}} \quad (1)$$

where  $Z_{\text{av}}$  is the average height for the entire region,  $Z_i$  is the height of individual point  $i$ , and  $N$  is the number of points measured within a given area.

Surface's wetting ability was investigated by static contact angle measurement (rame-hart Instrument Co.). De-ionized water was dropped on to the film's surface using a microsyringe. Photo of water droplet was recorded with a CCD camera, a curvature profile was created and then the contact angle measured. For each sample, the contact angle measurement was

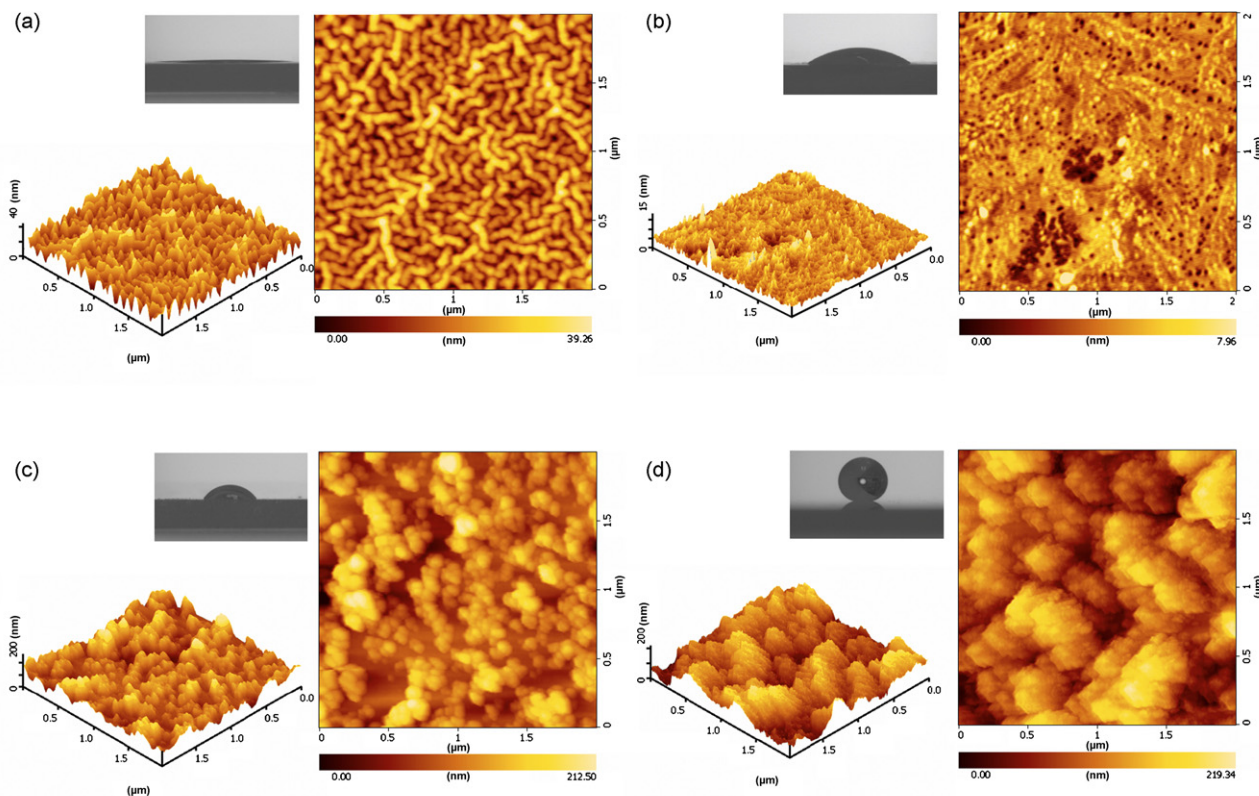


Fig. 1. 2D and 3D AFM topographical images of (a) polyelectrolyte film, (b) polyelectrolyte film etched for 60 min, (c) etched polyelectrolyte film coated with SiO<sub>2</sub> nanoparticles and (d) then coated with semifluorinated silane. A photo of water droplet on the specimen's surface is also included to reflect wetting characteristics.

performed on 10 different areas. The optical transmittance was determined by using the USB 4000 Ocean Optics spectrometer using a deuterium and halogen light source.

Anti-adhesion and self-cleaning properties were evaluated by applying red powder onto the specimen. After flipping over the sample to get rid off the dirt particles, the specimen's surface was preliminary observed with naked eyes and an optical microscope. In a separate experiment, several water droplets were applied onto the 45°-inclined specimen surface, and the surface was evaluated for dirt particle pick up by the water droplets.

### 3. Results and discussion

Fig. 1(a) shows AFM images of the as-prepared polyelectrolyte film before subjecting to chemical etching. Photo of water droplet on the film's surface recorded by using a CCD camera is also provided to reflect the film's wetting ability. A 2D topographical image revealed articulated worm-like structure of ~50–70 nm wide and ~0.5 μm long densely packed over the entire surface. Each articulated feature consisted of ~5–10 segments. A 3D topographical image clearly revealed that the film's surface consisted of protrusions of 20–30 nm high. The size of each protrusion was approximately the same size as each segment of the articulated features observed in the 2D image. The RMS roughness of this film was  $6.3 \pm 0.3$  nm. Water contact angle of this film was immeasurable since water completely wetted its surface indicating superhydrophilic characteristics. Surface topography significantly changed when the film was etched in HCl solution for 60 min as shown in Fig. 1(b). The articulated feature was etched away leaving behind ~30–50 nm dimples or open porosity seen as dark spots in a 2D image although few larger dimples were also present. A 3D image also

Table 1

Summary of the water contact angle and surface roughness of each layer

Sample	Contact angle (°)	RMS roughness (nm)
PAH_PAA	<5 <sup>a</sup>	$6.3 \pm 0.03$
PAH_PAA_Etch		
(15 min)	$39.3 \pm 4$	$1.8 \pm 0.01$
(60 min)	$45.3 \pm 3$	$1.8 \pm 0.01$
(180 min)	$36.8 \pm 2$	$3.3 \pm 0.02$
(420 min)	$48.0 \pm 2$	$4.1 \pm 0.02$
PAH_PAA_Etch_SiO <sub>2</sub>	$43 \pm 3$	$33.7 \pm 1.7$
PAH_PAA_Etch_SiO <sub>2</sub> _SFS	$152 \pm 4$	$39.1 \pm 2.0$

<sup>a</sup> Too low to be measurable.

revealed much finer surface roughness corresponding to RMS roughness of  $1.8 \pm 0.01$  nm. Such surface feature gave water contact angle of 45° which was much higher than that of the as-prepared film. According to Wenzel model, the contact angle of hydrophilic surface decreases with increasing roughness provided that the surface remains identical chemistry. However, the etched polyelectrolyte film in Fig. 1(b) behaved in the opposite trend probably as a result of surface chemistry modification after chemical etching.

Fig. 1(c) shows AFM topographical images of the polyelectrolyte film etched for 60 min, and then deposited with SiO<sub>2</sub> nanoparticles. The film's surface was covered with SiO<sub>2</sub> particles of around 50–100 nm in size. It was anticipated that the SiO<sub>2</sub> particles deposited onto the dimples of the etched surface as shown in Fig. 1(b). This film has the RMS roughness of 33.7 nm which was about the size of individual SiO<sub>2</sub> nanoparticle, and exhibited water contact angle of 43°. The superhydrophobic surface was achieved when the film was further coated with a semifluorinated silane which had low surface energy. It is suggested that fumed SiO<sub>2</sub> particle is hydrophilic since its surface

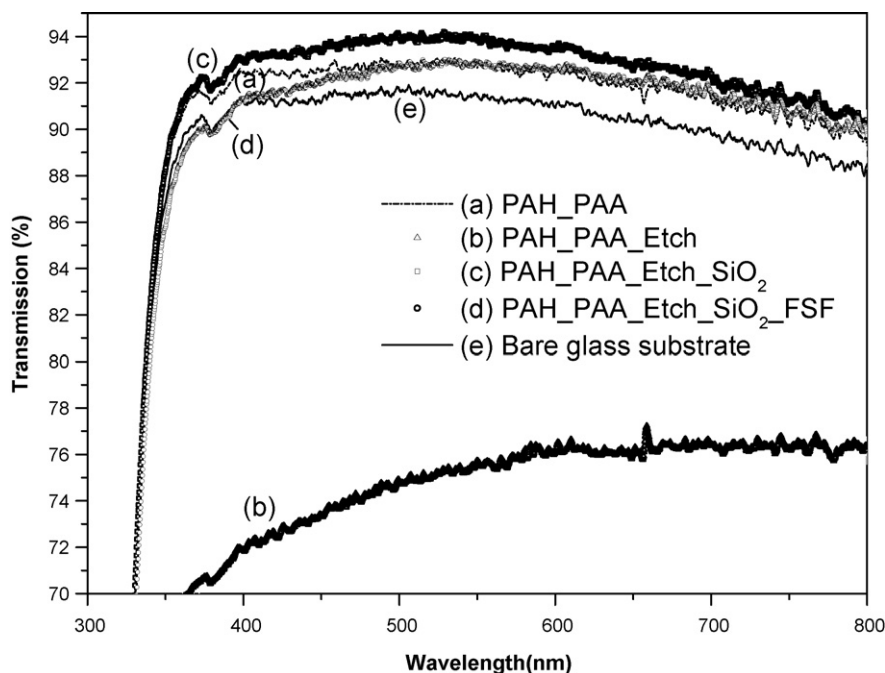


Fig. 2. Optical transmittance of (a) polyelectrolyte film, (b) polyelectrolyte film etched for 60 min, (c) etched polyelectrolyte film modified with fumed SiO<sub>2</sub> and (d) after coating with semifluorinated silane. The transmittance of bare substrate is shown in (e).

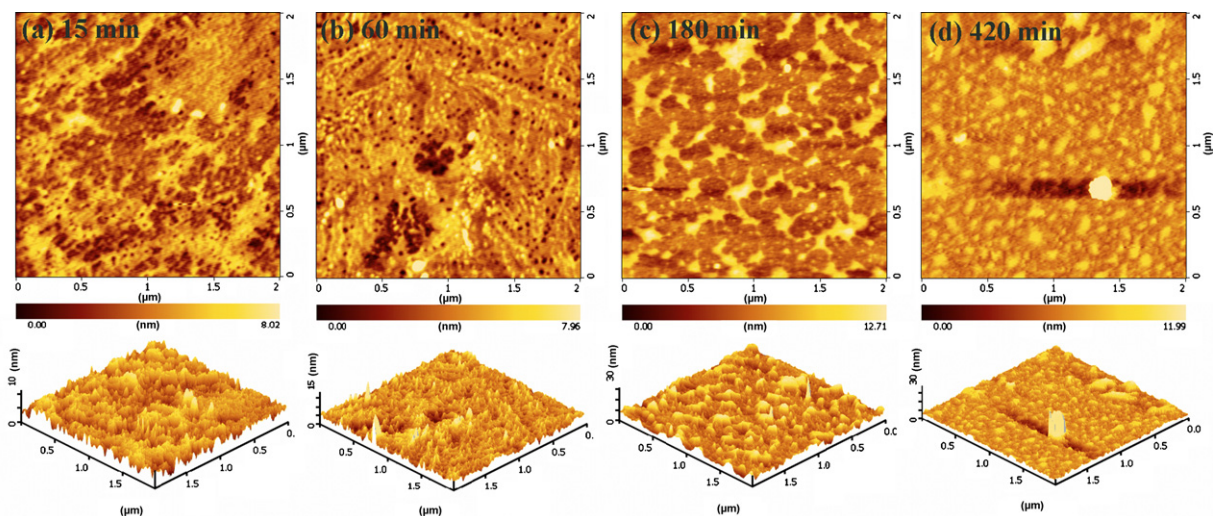


Fig. 3. AFM topographical images of the polyelectrolyte film etched at different times.

consisted of large number of hydroxyl groups. These surface hydroxyl groups reacted with a silane terminal group of the semifluorinated silane molecules, resulting in strong adhesion between the SiO<sub>2</sub> particle and the silane coating. Topographical images of this film shown in Fig. 1(d) revealed protrusions at sub-micrometer to micrometer scale, which was much larger than the roughness of the underneath film (polyelectrolyte film coated with SiO<sub>2</sub> particles). It is also seen from the 3D image that the protrusions consisted of much finer-scaled roughness attributed to the silane coating. Such double-scaled roughness surface feature was similar to that of lotus leaf. Its RMS roughness was 39 nm and exhibited contact angle of 152°. Values of contact angle and surface roughness of these films are summarized in Table 1.

Fig. 2 shows transmittance spectra of the as-prepared polyelectrolyte film, the film etched for 60 min, the etched film coated with SiO<sub>2</sub> nanoparticles and finally coated with a semifluorinated silane. The transmittance of the polyelectrolyte film was about 92% which was slightly higher than that of the bare glass substrate. Therefore, the film was transparent. The transmittance reduced to about 75% after etching. This etched film was slightly visually translucent. After coating the etched film with SiO<sub>2</sub> nanoparticles, the transmittance was raised back to about 93%. The transmittance decreased slightly after the silane coating, nevertheless it remained transparent. The transmittance of the films prepared in this work was closed to that of the optically transparent superhydrophobic films reported in the literature.<sup>13</sup>

To further investigate the effect of etching time on surface topography, the underlying polyelectrolyte films were etched for various times, i.e. 15–480 min. Surface topography of these films is shown in Fig. 3, and values of surface roughness and water contact angle summarized in Table 1. The films etched for 15 and 60 min essentially had similar surface topography and wetting ability. The surface characteristics obviously changed after etching for 180 min and longer as much larger hills and valleys were observed in the AFM images indicating more porous

surface. However, the RMS roughness only slightly increased while the wetting characteristics were basically unchanged.

Fig. 4 is a plot of the contact angle and surface roughness of the silane-coated hydrophobic films versus etching time of the polyelectrolyte bilayer. Both surface roughness and contact angle increased with the increase of etching time. The highest contact angle of 159° was obtained at the etching time of 420 min. The corresponding surface topography of this film is shown in Fig. 5. Note that values of RMS surface roughness of the hydrophobic films (~37–46 nm depending on etching time) were much higher than that of the etched polyelectrolyte bilayer (1.8–4.1 nm), and corresponded to the size of SiO<sub>2</sub> nanoparticle (40–45 nm). In this work, a superhydrophobic characteristics (contact angle ≥150°) was achieved by a combination of the increased surface roughness and surface modification with low surface free energy substance (a semifluorinated silane).

The results of self-cleaning and anti-adhesion properties are shown in Fig. 6. As shown in Fig. 6(a) and (b), much of the red

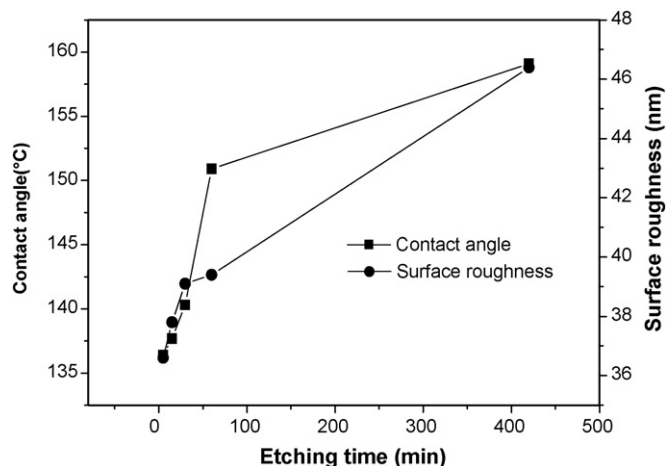


Fig. 4. A plot of water contact angle and surface roughness of the silane-coated hydrophobic films vs. etching time of the polyelectrolyte bilayer.

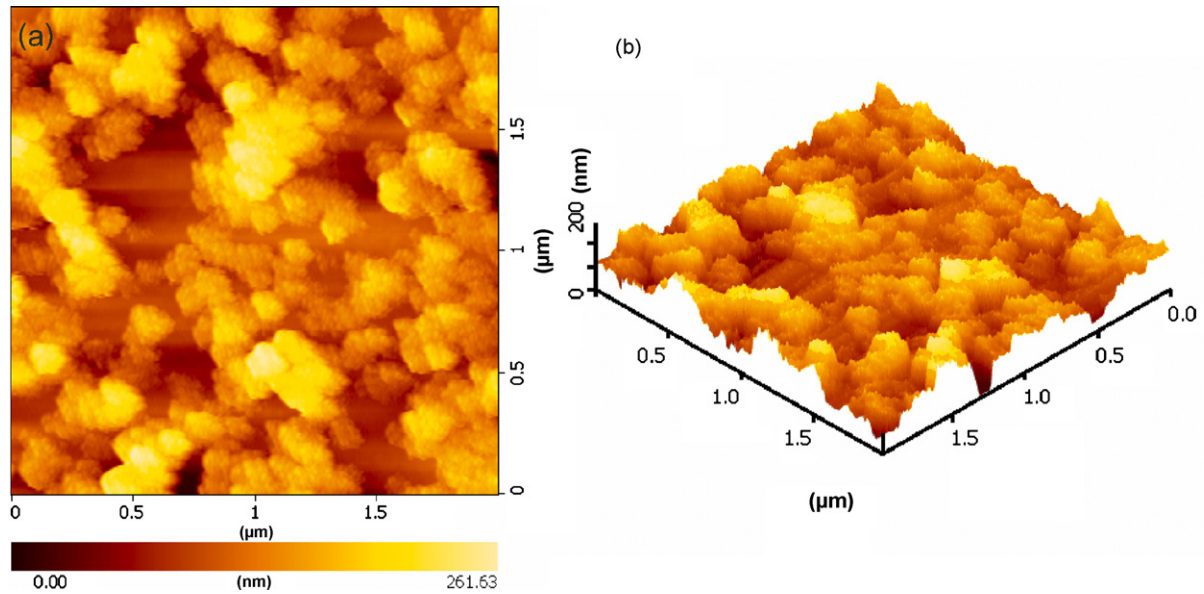


Fig. 5. AFM topographical images of the hydrophobic films prepared by etching the polyelectrolyte bilayer for 420 min. This film exhibited water contact angle of  $152^\circ$ .

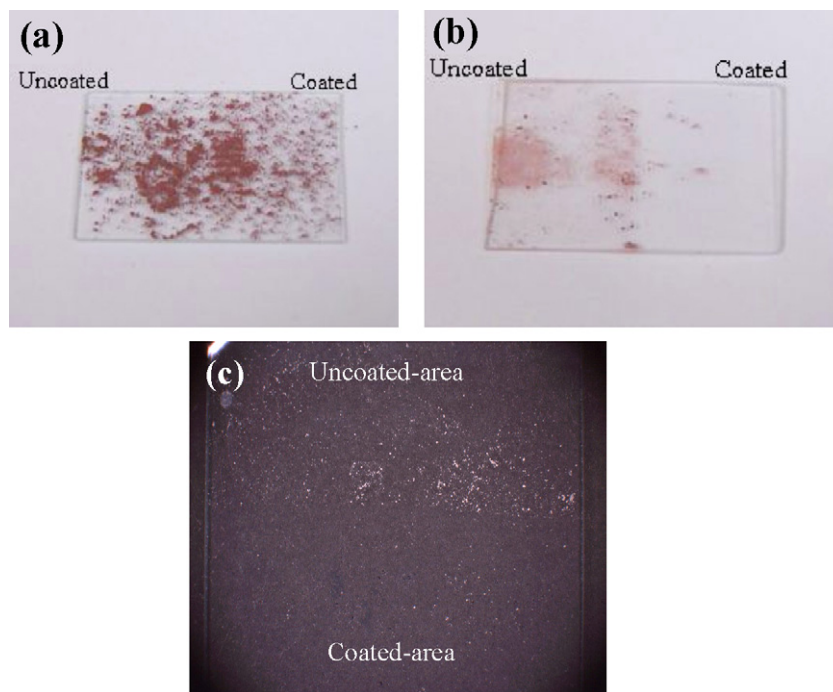


Fig. 6. (a) Photo of the uncoated and hydrophobic film-coated specimen with red powder sprinkled on the surface. (b) Photo of the same specimen after several water droplets were applied over the surface. (c) OM picture of dust particles left on the uncoated- and coated-surface after the dust was heavily applied to the specimen surface and then gently blown off.

powder was still spread on the uncoated surface after cleaning with water droplets, while the hydrophobic-coated surface was much cleaner although some powder still remained on the surface. Fig. 6(c) is an optical microscope picture of the uncoated area and the area coated with a superhydrophobic film after dust particles were heavily sprinkled on the specimen's surface and then were removed simply by flipping the sample. It is evident that much fewer dust particles adhered to the surface coated with

the superhydrophobic film exhibiting anti-adhesion property. Boundary between the two surfaces is clearly seen.

#### 4. Conclusions

Synthetic superhydrophobic surfaces have been fabricated through surface roughness enhancement by acid etching followed by surface modification with  $\text{SiO}_2$  nanoparticles and a

semifluorinated silane, respectively, by a dip coating method. The superhydrophobic films were optically transparent and had good anti-adhesion property. All the coating steps employed wet chemical process, and therefore simple and less expensive as no special equipment required. A scale up for large panel coating is also feasible with some modification of a dip coater.

### Acknowledgement

The financial of this research was supported by the National Metal and Materials Technology Center, the National Science and Technology Development Agency, Thailand (Grant # MT-B-49-ATO-07-020-I).

### References

1. Neinhuis, C. and Barthlott, W., Characterization and distribution of water-repellent, self-cleaning plant surfaces. *Ann. Bot.*, 1997, **79**, 667–677.
2. Kamitani, K. and Teranishi, T., Development of water-repellent glass improved water-sliding property and durability. *J. Sol-Gel Sci. Technol.*, 2003, **26**, 823–825.
3. Lin, T.-S., Wu, C.-F. and Hsieh, C.-T., Enhancement of water-repellent performance on functional coating by using the Taguchi method. *Surf. Coat. Technol.*, 2006, **200**, 5253–5258.
4. Burton, Z. and Bhushan, B., Hydrophobicity, adhesion, and friction properties of nanopatterned polymers and scale dependence for micro- and nanoelectromechanical systems. *Nano Lett.*, 2005, **5**, 1607–1613.
5. Zhang, H., Lamb, R. and Lewis, J., Engineering nanoscale roughness on hydrophobic surface—preliminary assessment of fouling behavior. *Sci. Technol. Adv. Mater.*, 2005, **6**, 236–239.
6. Ma, M. and Hill, R. M., Superhydrophobic surfaces. *Curr. Opin. Colloid Interface Sci.*, 2006, **11**, 193–202.
7. Zhang, J. L., Li, J. A. and Han, Y. C., Superhydrophobic PTFE surfaces by extension. *Macromol. Rapid Commun.*, 2004, **25**, 1105–1108.
8. Khorasani, M. T., Mirzadeh, H. and Kermani, Z., Wettability of porous polydimethylsiloxane surface: morphology study. *Appl. Surf. Sci.*, 2005, **242**, 339–345.
9. Lu, X. Y., Zhang, C. C. and Han, Y. C., Low-density polyethylene superhydrophobic surface by control of its crystallization behavior. *Macromol. Rapid Commun.*, 2004, **25**, 1606–1610.
10. Yang, Y. H., Li, Z. Y., Wang, B., Wang, C. X., Chen, D. H. and Yang, G. W., Self-assembled ZnO agave-like nanowires and anomalous superhydrophobicity. *J. Phys. Condens. Matter*, 2005, **17**, 5441–5446.
11. Lacroix, L. M., Lejeune, M., Ceriotti, L., Kormunda, M., Meziani, T., Colpo, P. *et al.*, Tuneable rough surfaces: a new approach for elaboration of superhydrophobic films. *Surf. Sci.*, 2005, **592**, 182–188.
12. Furstner, R., Barthlott, W., Neinhuis, C. and Walzel, P., Wetting and self-cleaning properties of artificial superhydrophobic surfaces. *Langmuir*, 2005, **21**, 956–961.
13. Shang, H. M., Wang, Y., Limmer, S. J., Chou, T. P., Takahashi, K. and Cao, G. Z., Optically transparent superhydrophobic silica-based films. *Thin Solid Films*, 2005, **472**, 37–43.
14. Zhai, L., Cebec, F. C., Cohen, R. E. and Rubner, M. F., Stable superhydrophobic coatings from polyelectrolyte multilayers. *Nano Lett.*, 2004, **4**, 1349–1353.